UNCLASSIFIED
(Approved for Publication)

CLM -P 19

THE EFFECTS OF AN ANISOTROPIC CONDUCTIVITY ON MAGNETIC FIELD DIFFUSION IN A STATIONARY PLASMA, AND AN APPLICATION TO THE INDUCED REVERSAL OF AN AXIAL FIELD

by

G. D. HOBBS

A B S T R A C T

The diffusion of magnetic fields into a cylindrical stationary plasma is considered. The effects of an anisotropic electrical conductivity, particularly in the limit $\sigma_\perp/\sigma_{11} \ll 1$, and of the time dependent terms are discussed. The use of steady state solutions to represent time dependent situations is shown to be justifiable unless $\sigma_\perp/\sigma_{11} \to 0$ and the ratio B_z/B_θ at any point becomes appreciably less than unity.

The coupled diffusion equations are integrated numerically and it is possible to predict, both qualitatively and quantitatively, the phenomena observed experimentally during the programmed reversal of the axial magnetic field in a slow pinch discharge.

It is suggested that this theory might be equally successful in interpreting other transient situations arising in cylindrical (or, to an approximation, toroidal) pinch discharges.

U.K.A.E.A. Research Group,
Culham Laboratory,
Nr. Abingdon,
BERKS.

May, 1963
(C/18)

1. INTRODUCTION

In recent years various authors[1-3] have reported that the magnetic field configurations observed in cylindrical and toroidal slow pinch discharges show a close resemblance to those derived from the steady state solutions of the equations describing the "Force Free Paramagnetic Model"[4]. These are a consequence of taking Maxwell's equations together with an ohms law in which the electrical conductivity is assumed anisotropic and proceeding to the limit $\sigma_\perp/\sigma_{11} = 0$, where $\sigma_\perp$ and σ_{11} are the conductivities perpendicular and parallel to the magnetic lines of force.

In this paper the same model is discussed, but with the force free and steady state restriction relaxed, the former being reimposed later. In order to illustrate the apparent applicability of the model to certain practical situations, calculations are reported which are directly comparable with the experimental results[3,5,6] resulting from the investigation of the phenomena observed during the programmed reversal of the axial magnetic field (B_z) in a toroidal pinch discharge. In these experiments magnetic field configurations were observed which did not correspond to any possible steady state solutions obtainable from this model, and in which transient effects were obviously of great importance.

In section 2 the theory, some of which is already well known, is outlined and in section 3 a précis of the latest published experimental results is presented. This is followed, in section 4, by a description of the results of the present calculations and a comparison is made with experiment. The main conclusions are

summarized in section 5.

2. THE FIELD DIFFUSION EQUATIONS

The equations applicable to this problem are Maxwell's equations in which displacement currents are neglected (MKS units),

$$\text{curl } \underset{\sim}{B} = \mu_o \underset{\sim}{j} \quad , \tag{1}$$

$$\text{curl } \underset{\sim}{E} = - \frac{\partial \underset{\sim}{B}}{\partial t} \quad , \tag{2}$$

$$\text{div } \underset{\sim}{B} = 0 \tag{3}$$

and ohms law

$$\underset{\sim}{j} = \sigma^{I} \underset{\sim}{E}_{11} + \sigma^{II} \underset{\sim}{E}_{1} + \sigma^{III} \frac{\underset{\sim}{B} \times \underset{\sim}{E}_{1}}{|B|}, \tag{4}$$

where $\underset{\sim}{E}_{11}$ and $\underset{\sim}{E}_{1}$ are the electric fields parallel and perpendicular to the magnetic field $\underset{\sim}{B}$ and σ^{I}, σ^{II} and σ^{III} are the components of the conductivity tensor.

The actual physical system described by these equations can be interpreted as a plasma with an anisotropic conductivity, for which inertial effects are negligible, and whose pressure gradient balances the $\underset{\sim}{j} \times \underset{\sim}{B}$ forces resulting from the currents and fields present within it. In the force free limit this pressure gradient must be zero and the plasma is effectively decoupled from the electro-magnetic fields, except in so far as the conductivity is a plasma property, and behaves essentially as a rigid conductor.

Since all other plasma properties remain undetermined by this set of equations there is no a priori reason for assuming σ^{I}, σ^{II} and σ^{III} to be spatially uniform. However this assumption, or more precisely that certain combinations are spatially uniform, is made in the calculations described below.

The region in which the equations are valid is taken to be an infinitely long cylinder of radius r_o described by cylindrical coordinates (r, θ, z), the z axis being directed along the axis of

the cylinder. The assumptions that all quantities are independent of θ and z and that the cylinder is encased by an ideally conducting wall, cut suitably to allow flux to enter and leave the system, lead, via Eq. (3), to $B_r = 0$. Similarly, since charge neutrality is required at all points, div $\underset{\sim}{j} = 0$, and hence $j_r = 0$. Under these conditions conductivities, parallel and perpendicular to the magnetic field, can be defined by[7]

$$\sigma_{11} = \sigma^{I}, \quad \sigma_{\perp} = \sigma^{II} + \frac{(\sigma^{III})^2}{\sigma^{II}} ,$$

and Eq. (1)-(4) can be written in the form

$$j_z = \frac{1}{\mu_o} \frac{1}{r} \frac{\partial}{\partial r} (rB_\theta) , \tag{5}$$

$$j_\theta = - \frac{1}{\mu_o} \frac{\partial B_z}{\partial r} , \tag{6}$$

$$\frac{\partial E_z}{\partial r} = \frac{\partial B_\theta}{\partial t} , \tag{7}$$

$$\frac{1}{r} \frac{\partial}{\partial r} (r E_\theta) = - \frac{\partial B_z}{\partial t} , \tag{8}$$

$$E_\theta = \mu_o (\eta_{zz} j_\theta + \eta_{z\theta} j_z) , \tag{9}$$

$$E_z = \mu_o (\eta_{\theta z} j_\theta + \eta_{\theta\theta} j_z) , \tag{10}$$

where

$$\eta_{zz} = \frac{1}{\mu_o \sigma_{11}} \left[1 + \frac{(\sigma_{11} - \sigma_\perp)}{\sigma_\perp} \left(\frac{B_z}{B}\right)^2 \right] , \tag{11}$$

$$\eta_{\theta\theta} = \frac{1}{\mu_o \sigma_{11}} \left[1 + \frac{(\sigma_{11} - \sigma_\perp)}{\sigma_\perp} \left(\frac{B_\theta}{B}\right)^2 \right] \tag{12}$$

and

$$\eta_{\theta z} = \eta_{z\theta} = - \frac{1}{\mu_o \sigma_{11}} \frac{(\sigma_{11} - \sigma_\perp)}{\sigma_\perp} \frac{B_\theta B_z}{B^2} , \tag{13}$$

$$B^2 = B_z^2 + B_\theta^2 .$$

The radial component of the electric field is determined from the condition $j_r = 0$ and is given by

$$E_r = \frac{\sigma^{III}}{\sigma^{II}} \frac{B_z E_\theta - B_\theta E_z}{|B|}$$

These equations can be combined to yield the magnetic field diffusion equations

$$\frac{\partial B_z}{\partial t} = \frac{1}{r}\frac{\partial}{\partial r}\left[\eta_{zz}\, r \frac{\partial B_z}{\partial r} - \eta_{z\theta}\frac{\partial}{\partial r}(r B_\theta)\right] \qquad (14)$$

and

$$\frac{\partial B_\theta}{\partial t} = \frac{\partial}{\partial r}\left[-\eta_{\theta z}\frac{\partial B_z}{\partial r} + \eta_{\theta\theta}\frac{1}{r}\frac{\partial}{\partial r}(r B_\theta)\right] . \qquad (15)$$

It should be noted that the subscripts on η have been chosen to give a symmetric form to these equations, and equations (11)-(13), and not to (9) and (10) as is more usual.

Equations (5)-(15) describe the behaviour of the model in the most general terms and it is instructive to investigate a number of limiting conditions which may be applicable to particular situations.

(i) Isotropic Conductivity

If the conductivity is assumed isotropic, i.e. $\sigma_{11} = \sigma_{\perp} = \sigma$, then

$$\eta_{zz} = \eta_{\theta\theta} = 1/\mu_o\sigma ,$$

and

$$\eta_{z\theta} = \eta_{\theta z} = 0.$$

The magnetic field diffusion equations decouple giving independent equations for each component:

$$\left.\begin{aligned} \frac{\partial B_z}{\partial t} &= \frac{1}{\mu_o\sigma}\frac{1}{r}\frac{\partial}{\partial r} r \frac{\partial B_z}{\partial r} \\ \text{and} \quad \frac{\partial B_\theta}{\partial t} &= \frac{1}{\mu_o\sigma}\frac{\partial}{\partial r}\frac{1}{r}\frac{\partial}{\partial r}(r B_\theta) . \end{aligned}\right\} \qquad (16)$$

Both have a characteristic diffusion time $\tau = \mu_o\, r_o^2\, \sigma$. Analytic solutions of these equations have been obtained by a number of authors, both for this cylindrical case[8,9], and for a toroidal conductor[10].

(ii) Force Free Fields

By definition force free fields satisfy the condition $\underset{\sim}{j} \times \underset{\sim}{B} = 0$. Inversion of Eq.(9) and (10) gives

$$\left.\begin{aligned} j_z &= (\sigma_{11} - \sigma_\perp)(B_z/B^2)\ (B_z E_z + B_\theta E_\theta) + \sigma_\perp E_z\ , \\ j_\theta &= (\sigma_{11} - \sigma_\perp)(B_\theta/B^2)\ (B_z E_z + B_\theta E_\theta) + \sigma_\perp E_\theta\ . \end{aligned}\right\} \qquad (17)$$

Since $B_r = 0$, $\underset{\sim}{j} \times \underset{\sim}{B}$ has only a radial component which is given by

$$(\underset{\sim}{j} \times \underset{\sim}{B})_r = \sigma_\perp (B_z E_\theta - B_\theta E_z).$$

If $\sigma_\perp = 0$ this is necessarily zero.

If $B_z E_\theta - B_\theta E_z$ vanishes it is consequential that B_θ and B_z must be coupled at the boundary $r = r_o$, i.e. a specification of $B_\theta(r_o, t)$ uniquely determines $B_z(r_o, t)$ and vice versa. Since in most experimental situations these fields are produced by independent mechanisms, the condition $B_z E_\theta - B_\theta E_z = 0$ will in general be too restrictive and cannot be considered. Thus, within the framework of this model, the condition $\underset{\sim}{j} \times \underset{\sim}{B} = 0$ and $\sigma_\perp = 0$ are synonymous.

Further properties of force free fields will be considered in a later paragraph, with particular reference to steady state configurations.

(iii) Small B_θ

If $B_\theta/B_z \ll 1$, Eq.(11)-(13) can be approximated by

$$\eta_{zz} \approx \frac{1}{\mu_o \sigma_\perp}\left[1 - (\frac{B_\theta}{B_z})^2 \frac{\sigma_{11} - \sigma_\perp}{\sigma_{11}}\right],$$

$$\eta_{\theta\theta} \approx \frac{1}{\mu_o \sigma_{11}}\left[1 + (\frac{B_\theta}{B_z})^2 \frac{\sigma_{11} - \sigma_\perp}{\sigma_\perp}\right],$$

$$\eta_{z\theta} = \eta_{\theta z} \approx -\frac{1}{\mu_o \sigma_{11}} (\frac{B_\theta}{B_z}) \frac{\sigma_{11} - \sigma_\perp}{\sigma_\perp}\ .$$

Thus if "small B_θ" is defined in the sense

$$|\frac{B_\theta}{B_z}| \ll \frac{\sigma_\perp}{\sigma_{11} - \sigma_\perp}\ , \qquad (18)$$

then

$$\eta_{zz} \approx 1/\mu_o \sigma_\perp ,$$

$$\eta_{\theta\theta} \approx 1/\mu_o \sigma_{11} ,$$

$$\eta_{z\theta} = \eta_{\theta z} \approx 0$$

and again the diffusion equations decouple to give

$$\left.\begin{aligned} \frac{\partial B_z}{\partial t} &= \frac{1}{\mu_o \sigma_\perp} \frac{1}{r} \frac{\partial}{\partial r} r \frac{\partial B_z}{\partial r} \\ \text{and} \qquad \frac{\partial B_\theta}{\partial t} &= \frac{1}{\mu_o \sigma_{11}} \frac{\partial}{\partial r} \frac{1}{r} \frac{\partial}{\partial r} (rB_\theta). \end{aligned}\right\} \qquad (19)$$

Now B_θ diffuses with a characteristic time $\tau_{11} = \mu_o \sigma_{11} r_o^2$ and B_z with a characteristic time $\tau_\perp = \mu_o \sigma_\perp r_o^2$. If $\sigma_\perp$ is small, i.e. near the force free limit, the possibility of very rapid diffusion of B_z becomes apparent. This fact is of particular importance at $r = 0$, where in cylindrical systems $B_\theta/B_z \rightarrow 0$, and is discussed in more detail in later paragraphs. It should be noted however that the smaller $\sigma_\perp/\sigma_{11}$ becomes the more rapidly B_z can diffuse relative to B_θ but the more limited is the region over which it is able to do so, the region in question being that over which the inequality (18) remains unviolated.

(iv) Small B_z

Considerations similar to those of the preceding paragraph lead, if $|B_z/B_\theta| \ll \sigma_\perp/(\sigma_{11} - \sigma_\perp)$, to the diffusion equations

$$\left.\begin{aligned} \frac{\partial B_z}{\partial t} &= \frac{1}{\mu_o \sigma_{11}} \frac{1}{r} \frac{\partial}{\partial r} r \frac{\partial B_z}{\partial r} \\ \text{and} \qquad \frac{\partial B_\theta}{\partial t} &= \frac{1}{\mu_o \sigma_\perp} \frac{\partial}{\partial r} \frac{1}{r} \frac{\partial}{\partial r} (rB_\theta). \end{aligned}\right\} \qquad (20)$$

The roles of τ_{11} and $\tau_\perp$ are now interchanged and the possibility of rapid diffusion of B_θ can be considered. This condition will be of particular significance in field configurations possessing a partially reversed axial field.

(v) Steady State Fields

As indicated in the introduction, this class of solutions has been extensively studied by a number of authors[1-4,11]. However it is included here, partly for completeness, but mainly in order to make use of a particular property in the following discussion of the theoretical and experimental results.

The equations for the magnetic fields can be written in the following dimensionless form:

$$\frac{1}{x}\frac{d}{dx}(xb_\theta) = \frac{b_z^2}{b_\theta^2 + b_z^2} + \frac{\sigma_\perp}{\sigma_{11}}\frac{b_\theta^2}{b_\theta^2 + b_z^2} \quad , \tag{21}$$

$$-\frac{db_z}{dx} = \left(1 - \frac{\sigma_\perp}{\sigma_{11}}\right)\frac{b_\theta\, b_z}{b_\theta^2 + b_z^2} \quad , \tag{22}$$

where

$$b_z = B_z(r)/B_z(o) \ ,$$

$$b_\theta = B_\theta(r)/B_z(o) \ ,$$

$$x = r/r'$$

and

$$r' = B_z(o)/(\mu_o\, \sigma_{11}\, E_z) .$$

$B_z(o)$ is the value of B_z at $r = 0$ and E_z is the spatially uniform axial electric field ($E_\theta \equiv 0$). The boundary conditions are $b_\theta = 0$ and $b_z = 1$ at $x = 0$. Solutions for a number of values of $\sigma_\perp/\sigma_{11}$ are shown in Fig.1.

It will be observed that b_z does not change sign at any value of x for any value of $\sigma_\perp/\sigma_{11}$. Reference to Eq.(22) sheds some light on this observation, since, on dividing throughout by b_z and integrating once with respect to x, b_z can be written

$$b_z(x) = \exp - \int_o^x (1 - \sigma_\perp/\sigma_{11})\ b_\theta/b^2\ dx' \ ,$$

a form which is always positive.

It may also be shown that the asymptotic solution of Eq.(21) is

$$b_\theta \sim \frac{\text{const}}{x} + \frac{\sigma_\perp}{\sigma_{11}}\frac{x}{2} \ .$$

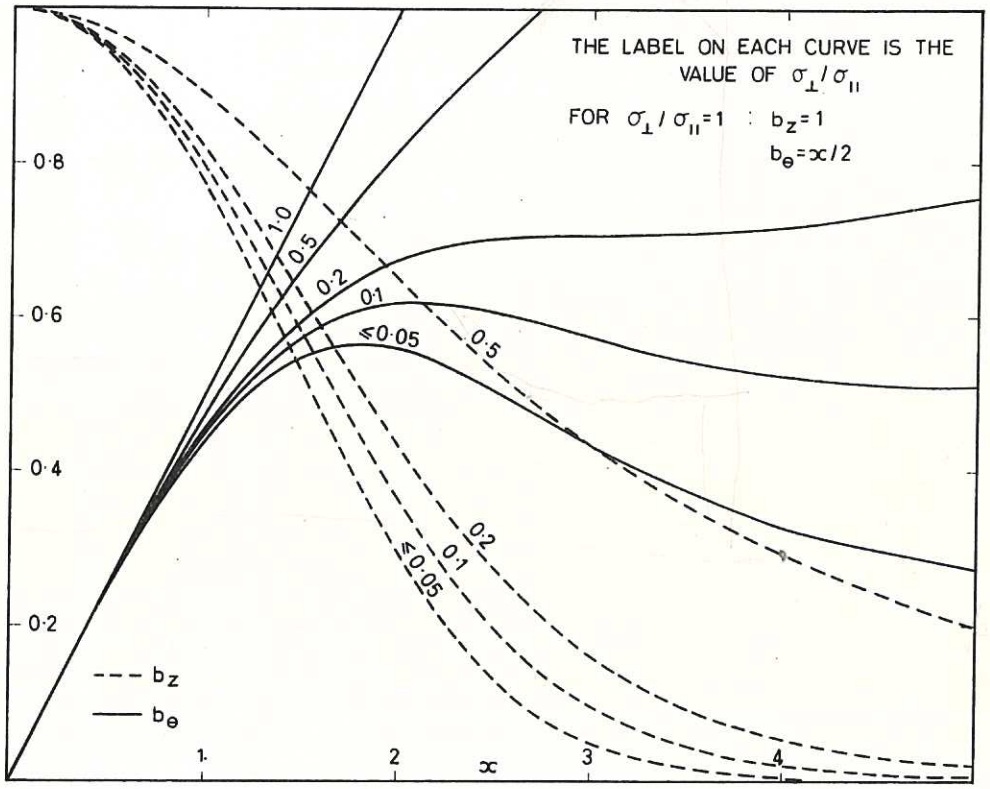

Fig. 1

Steady state solutions for various values of $\sigma_\perp/\sigma_{11}$

If $\sigma_\perp = \sigma_{11}$, the constant is zero. If $\sigma_\perp/\sigma_{11} \equiv 0$, b_θ tends to zero as $1/x$, but otherwise, for sufficiently large x, b_θ has a minimum (or perhaps just a region of reduced gradient) and thereafter increases linearly. The linear rise represents the current, $j_z = \sigma_\perp E_z$, due to the spatially uniform E_z and non-zero $\sigma_\perp$. This feature can be seen in Fig.1.

During the discussion of an experimental situation in a later section the behaviour of B_z on the axis, $r = 0$, as a function of B_θ and B_z at the wall, $r = r_o$, will be of particular interest. As a preliminary it is of value to investigate this relationship in the case of steady state fields. For a given $\sigma_\perp/\sigma_{11}$ the dependence of $B_z(o)/B_\theta(r_o)$ on $B_z(r_o)/B_\theta(r_o)$ can be expressed in a unique curve (Fig.2). A number of general points of interest arising from Fig.2 should be noted: (a) If $B_z(r_o)/B_\theta(r_o) \gg 1$, $B_z(o)$ and $B_z(r_o)$ are approximately equal, i.e. B_z is nearly uniform over the cross-section of the cylinder. (This may also be deduced from Eq.(18)); (b) if $0.2 \lesssim \sigma_\perp/\sigma_{11} \leqslant 1$, the dependence is monotonic; (c) if $0 < \sigma_\perp/\sigma_{11} \lesssim 0.2$ the variation has a minimum at $B_z(r_o)/B_\theta(r_o) \sim 1$ and a maximum when this quantity is small. The height of the maximum tends to infinity as $\sigma_\perp/\sigma_{11} \longrightarrow 0$; (d) if $\sigma_\perp/\sigma_{11} \equiv 0$, the maximum is non-existent and, for any finite $B_\theta(r_o)$, $B_z(o) \longrightarrow \infty$ as $B_z(r_o) \longrightarrow 0$. As stated in the introduction steady state solutions are frequently used for comparison with experimentally observed cylindrical (or toroidal) field configurations. At the present time the latter are seldom truly steady state phenomena and it is of interest to ask when such a comparison may justifiably be made. One answer to this question can be phrased as follows. Firstly, any field configuration exhibiting a reversed axial field is immediately excluded. Secondly, if, as is usually the case, time variation of the fields is initiated from the wall, then a slow imposed variation must

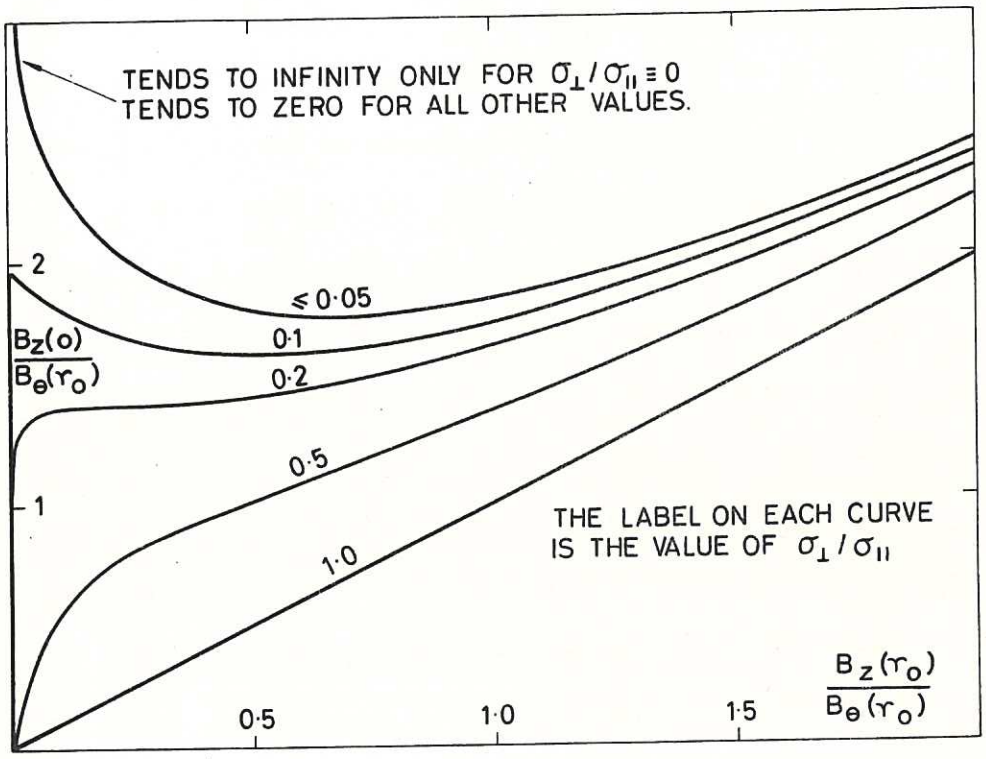

Fig. 2

The dependence of B_z at the centre on B_z and B_θ at the wall in the steady state approximation

itself produce only slow variations elsewhere. In this context "slow variation" means variation over times of the order of, or long compared to, any local resistive diffusion time (e.g. τ_{11} or $\tau_{\perp}$). From Fig.2 it becomes apparent that only if $\sigma_{\perp}/\sigma_{11} \gtrsim 1/2$ or $B_z(r_o)/B_\theta(r_o) \gtrsim 1$ will this condition be satisfied, for, if the contrary is true, a small change in $B_z(r_o)$, say, would tend to induce a large change in $B_z(o)$ in the same time interval. It would appear that this situation would be worst in the limit $\sigma_{\perp}/\sigma_{11} \longrightarrow 0$ but it is relieved to a certain extent, although not entirely removed, due to the relevant diffusion time for $B_z(o)$ being $\tau_{\perp}$. Thus, in general, field configurations possessing a partially reversed axial field or, if $\sigma_{\perp}/\sigma_{11}$ is small, a $B_z(r_o)/B_\theta(r_o) \ll 1$, cannot be safely discussed in terms of steady state solutions.

(vi) General Solutions

If the impressed field variation and its consequences are to be described accurately in circumstances that cannot be considered "slow", the full time-dependent equations, (14) and (15), must be solved. Due to their non-linearity an analytic approach is, in general, not very fruitful and it is necessary to resort to numerical methods. An implicit finite difference technique[12] has been adopted and programmed for the IBM 7090/7030 computers. Since the results of the calculations rather than the means of obtaining them constituted the motivation of this report, the details of the numerical analysis have been omitted.

Quite general boundary conditions were employed, of the form

(a) $B_\theta(r) = 0$ at $t = 0$, all $r \leqslant r_o$;

(b) $B_z(r) = B_{zo}$ at $t = 0$, all $r \leqslant r_o$;

(c) $B_\theta(r_o)$, or total axial current I, given as a function of time for $t > 0$;

(d) $B_z(r_o)$ given as a function of time for $t > 0$.

There is obviously an infinity of possible situations that could be analysed with such a programme but unlike an analytic approach it is not possible to present a general solution for these. In the rest of this paper attention is concentrated on a particular situation which has recently been the subject of a series of experiments. Thus the calculations, besides illustrating some of the complicated behaviour obtainable from these non-linear equations, take on a greater physical interest when compared with the experimental work.

3. PRÉCIS OF EXPERIMENTAL RESULTS

The experiments have in general been carried out on toroidal pinch devices which have facilities for applying an initial steady axial magnetic field B_z and an additional alternating axial field[3,5,6]. The sequence of operations varied from experiment to experiment but that period which is of concern here was little influenced by the exact details of this sequence. It is sufficient to state that at some stage in the discharge there existed a plasma carrying an axial current I distributed over the cross-section with density j_z, and containing a distributed axial magnetic field $B_z(r)$ with its associated j_θ. At a subsequent stage the value of B_z at the wall, $r = r_o$, was reduced to zero and made to change sign by the discharge of an auxiliary condenser bank through a solenoidal coil wound inside the conducting shell of the torus. Ultimately the B_z reversed in direction throughout the entire cross-section and it is the analysis of the phenomena observed during this process that is the concern of the following sections.

The observed sequence of events can be set out as follows: (References indicate the authors observing each feature).

If, initially, the axial field at the wall $B_z(r_o)$ was significantly greater than $B_\theta(r_o)$, then, as $B_z(r_o)$ was reduced in magnitude, the axial field at the centre of the cross-section was seen to decrease in phase[5]. When $B_z(r_o)$ became approximately equal to $B_\theta(r_o)$, at time t_1 (Fig.3), and while it was reduced further until it approached zero, $B_z(o)$ was seen to rise or at least remain approximately constant[5,6]. Simultaneously there was a redistribution of the axial current, the density near the wall being reduced with an enhancement of that near the centre[6]. When $B_z(r_o)$ reversed, $B_z(o)$ firstly continued its trend to rise or remain constant and then abruptly changed sign, the instant t_2 at which it passed through zero being delayed relative to the zero of $B_z(r_o)$ by a time $\delta\tau$ [5,6]. During this interval of time B_z was positive near the centre and negative near the wall. Its zero, which was accompanied by large radial gradients[6] in B_z and a local peak[6] in B_θ, was seen to move rapidly inwards and on reaching the centre gave rise to the abrupt reversal of B_z there.

These were the qualitative features observed. In addition certain quantitative results have been published by Babichev et al.[5]. In their experiments both the current I (i.e. $B_\theta(r_o)$) and the applied axial magnetic field ($B_z(r_o)$) were periodic in time and had fixed but different periods. They have reported the variation of the parameters $\tau = t_2 - t_1$ and ΔB_z, the value of $B_z(o)$ during the interval τ (Fig.3), with both the amplitude of the current pulse, I_{max}, and the maximum rate of change of the applied B_z (which is proportional to the amplitude, $B_{z\,max}$, at constant period). Their results are reproduced in Figures 9-11.

4. THEORETICAL RESULTS

A complete series of calculations has been done in which the boundary conditions on B_θ and B_z were taken to correspond, as accurately as possible, to those employed by Babichev et al.

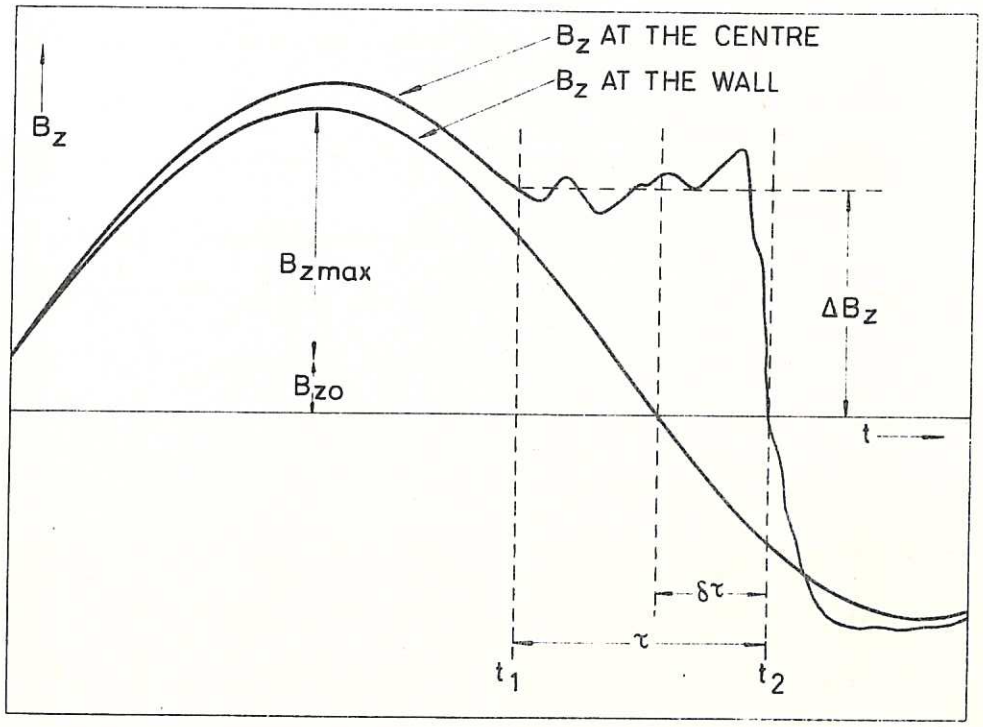

Fig. 3

Typical experimental variation with time of B_z at the centre and at the wall. B_{zo} is the initial axial field and B_{zmax} is the amplitude of the alternating axial field. ΔB_z is the mean value of B_z at the centre over the time interval τ. (Based on published oscillograms. See footnotes 3 and 5)

in their experiments. These experiments were carried out, as stated in the previous section, in a toroidal discharge tube. The calculations on the other hand have been done for an infinitely long cylindrical system and in all subsequent comparisons this inadequacy will be ignored.

The first half of this section will be devoted to a qualitative description of just one of these calculations. The physical interpretation of the phenomena occurring will be discussed in the appendix. The second half will be devoted to a quantitative analysis of the parameters equivalent to t_1, t_2, τ, $\delta\tau$ and ΔB_z derived from the complete series of calculations.

(i) Qualitative Results

The initial conditions for the case considered here were B_z uniform ($= B_{zo}$) and $B_\theta = 0$, for all r. The ratio of the conductivities $\sigma_\perp/\sigma_{11}$ was 0.05 which, to a good approximation, can be considered to be zero. The imposed boundary variation of B_θ and B_z was sinusoidal, B_θ oscillating about zero, B_z oscillating about B_{zo}. The relative periods for these oscillations are best appreciated by reference to Fig.4 in which $B_z(r_o)$ and $B_\theta(r_o)$ are plotted as functions of t/τ_{11}, where $\tau_{11} = \mu_o \sigma_{11} r_o^2$. For the purposes of a qualitative discussion the relative magnitudes of the fields, the normalized time t/τ_{11} and $\sigma_\perp/\sigma_{11}$ are the only parameters of any importance. The figure also displays the time variation of $B_z(o)$ computed both from a succession of steady state configurations and from the full time-dependent theory.

The first important point to note is that if $B_z(r_o) \gtrsim B_\theta(r_o)$ the two methods of calculation are in good agreement, but if the contrary is true they are widely divergent. The steady state configurations are totally inadequate to describe the field behaviour in the neighbourhood of $B_z(r_o)/B_\theta(r_o) = 0$. This illustrates, by practical verification, the validity of the criterion developed

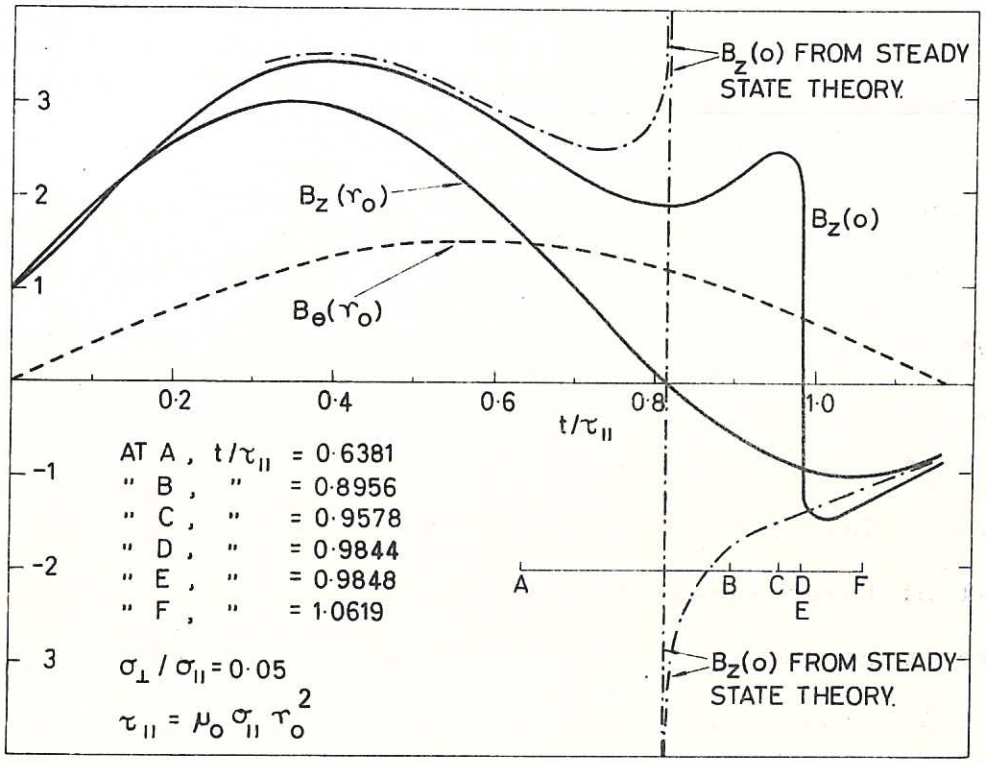

Fig. 4

Typical theoretical variation with time of B_z at the centre and at the wall. All fields have been normalized to the initial axial field B_{zo}. The variation of B_z at the centre is shown for both the steady state approximation (— . — .) and the full time dependent computation (————)

in section 2(v). A further point of minor interest is that, in the steady state approximation, $B_z(o)$ does pass through zero in a continuous manner. This would not be so if $\sigma_\perp/\sigma_{11} \equiv 0$ (Fig.2); it would tend positively to infinity on one side and negatively from infinity on the other.

The second point of importance is the close resemblance between $B_z(o,t)$ and the variation of this quantity observed experimentally (Fig.3). It shows the same tendency to rise as $B_z(r_o)$ passes through zero (conditions could have been chosen in which the rise would have been almost completely suppressed), followed by a delayed but very abrupt fall through zero to negative values. The time taken for this reversal is very short compared with τ_{11}.

Figures 5-8 illustrate the spatial distribution of fields and currents during the interesting period A to F defined in Fig.4. The first of these shows that the B_z profiles develop gradients which are large compared to those of the near equilibrium configuration at A. The resulting j_θ is shown in Fig.6 and demonstrates the existence of θ current densities which can rise to as much as 20 times the mean axial current density. In Fig.7 the behaviour of B_θ is shown, the most striking feature being the development of a sharp peak moving inwards from the wall to the centre. As would be expected, the j_z derived from these profiles is rather complicated. However, Fig.8 shows that the dominant behaviour is for the axial current to be constrained to a small central region of the cross-section, the value at r = 0 soaring to the order of 50 times the mean. At the boundary of this central core there is a well defined minimum which, in this case (it is not always so), is actually negative, i.e. there exists for a short time an annulus of current flowing in the opposite direction to the net current. This minimum and its associated B_θ peak possess a strong temporal and

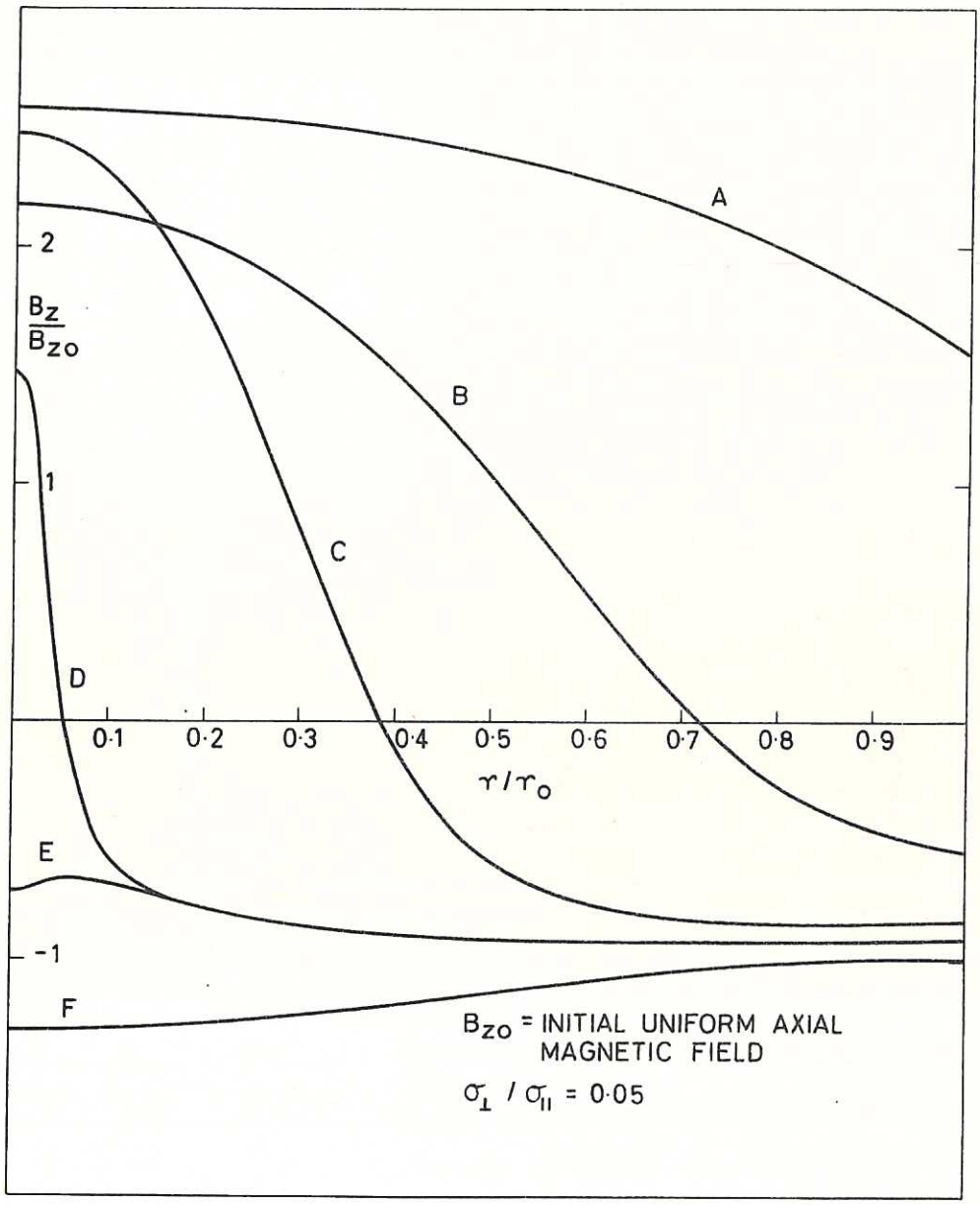

Fig. 5

The variation of B_z with radius computed at a number of successive times. (See Fig.4 for the definition of A, B, etc.)

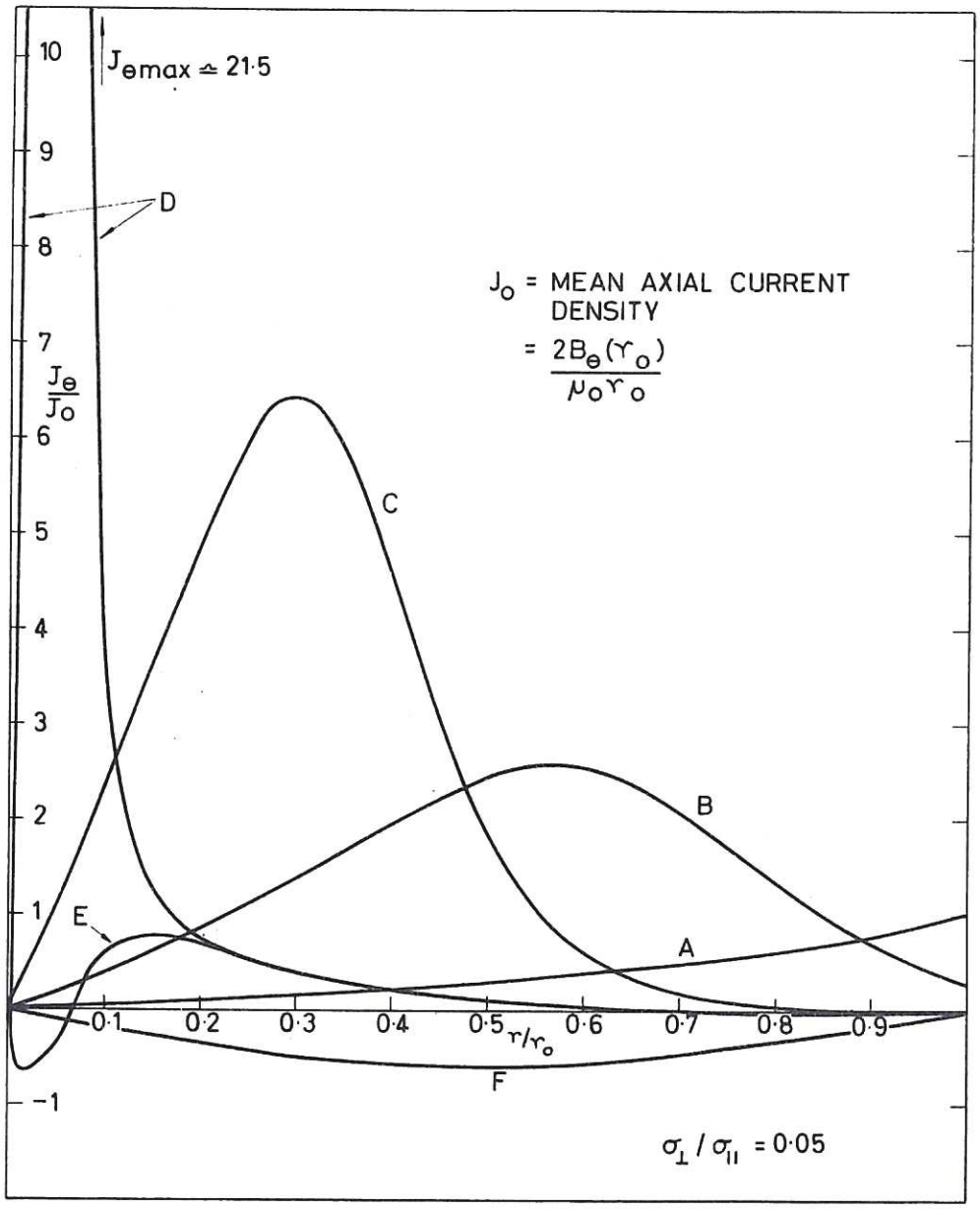

Fig. 6

The variation of J_θ with radius computed at a number of successive times. (See Fig.4 for the definition of A, B, etc.)

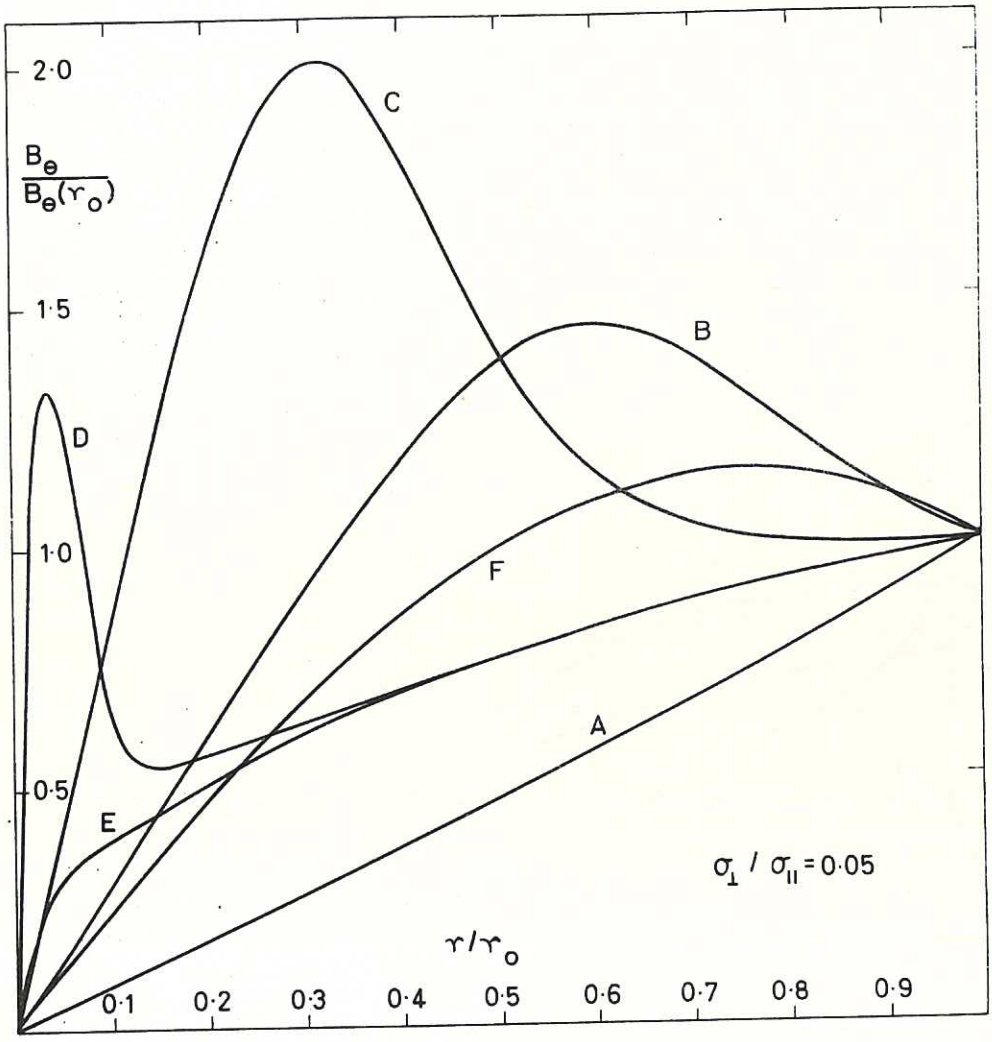

Fig. 7

The variation of B_θ with radius computed at a number of successive times. (See Fig.4 for the temporal variation of $B_\theta(r_o)$ and for the definition of A, B, etc.)

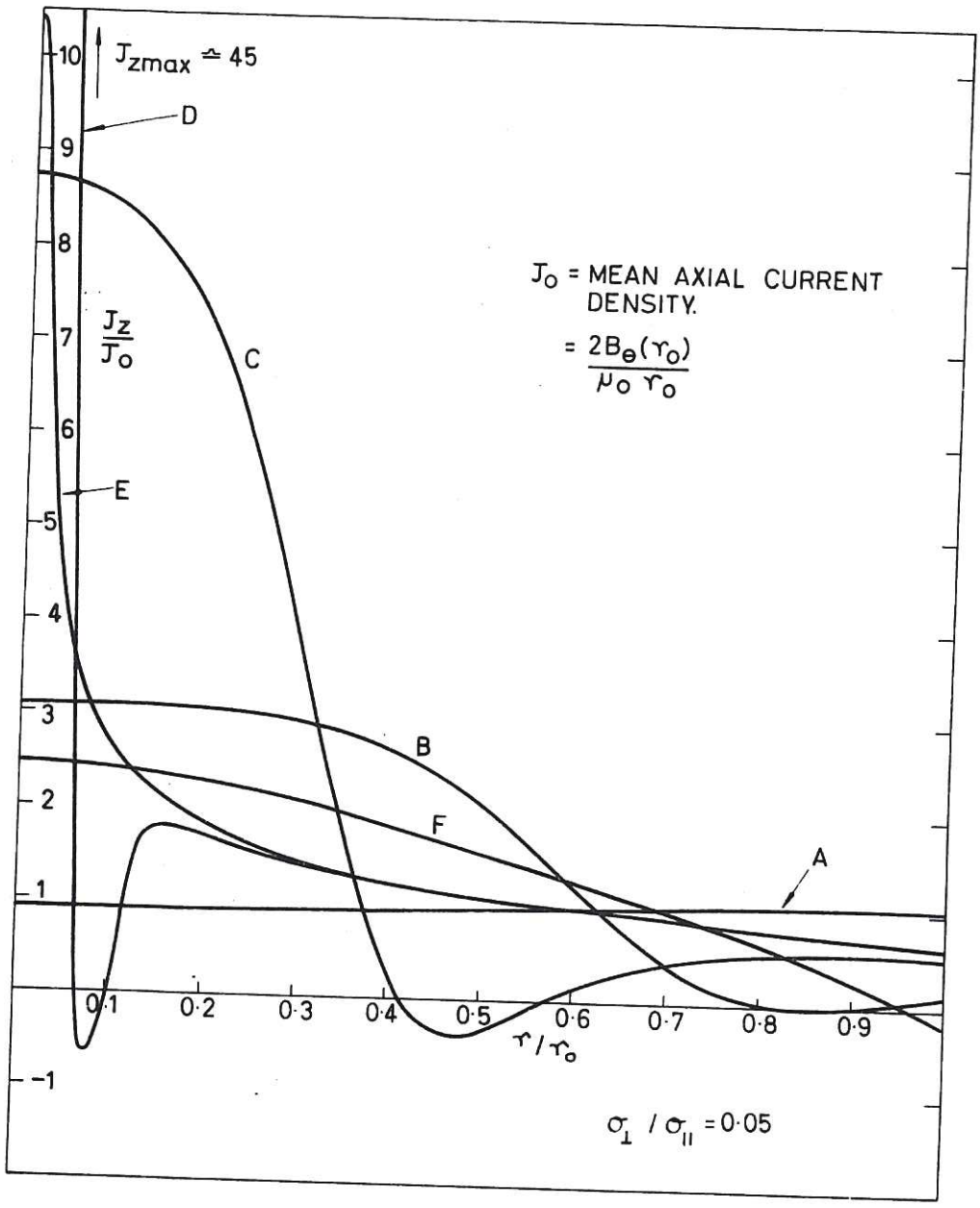

Fig. 8

The variation of J_z with radius computed at a number of successive times. (See Fig.4 for the temporal variation of $B_\theta(r_o)$ and for the definition of A, B, etc.)

spatial correlation with the zero of B_z.

These then are the qualitative features to be observed from the calculations taking into account the all-important transient terms. The physical processes underlying these results are discussed in some detail in the appendix. There is little need to emphasise the remarkable similarity in this case between theory and experiment. The calculations predict all the phenomena observed experimentally and it is by no means unreasonable to conclude that the time-dependent force free paramagnetic model is sufficient, at least in a qualitative manner, to account for the reported behaviour of a cylindrical pinch discharge subjected to field programming of this type.

(ii) Quantitative Results

It will have been observed from the preceding paragraphs that the details of an individual calculation are complex. In order to discuss a number of these, in which various parameters have been varied, in any concise manner, most of the detail must be omitted, attention being focussed on the dominant features. For this reason, and in order to make a direct comparison with experiment, the following paragraphs will be devoted to the temporal variation of B_z at the centre in relation to its variation at the wall and the variation of the current ($B_\theta(r_o)$). To facilitate the analysis, a number of constants, independent and dependent variables must be defined (Fig.3).

Constants:

In all the calculations reported the following set of constant parameters was used[5].

r_o = 8 cms

B_{zo} = 500 gauss

Applied B_z period = 240 μsecs

Current period = 400 μsecs

$\sigma_\perp/\sigma_{11}$ = 0.05

σ_{11} = 214 (ohms-cms)$^{-1}$

The last, σ_{11}, was calculated[13] assuming an electron temperature of 5 eV.

Independent variables:

The two quantities under direct control in the experiments were

I_{max} = Maximum value of the current (10-50 kamp)

and B_{zmax} = Maximum value of the applied alternating $B_z(r_o)$ (0.5-3.0 kgauss).

Consequently these parameters were varied within the ranges indicated.

Dependent variables:

For each combination of the above variables the following parameters were derived from the computed results.

t_1 = Time at which $B_z(r_o) = B_\theta(r_o)$

t_2 = Time at which $B_z(o) = 0$

$\tau = t_2 - t_1$

$\delta\tau$ = t_2 - (Time at which $B_z(r_o) = 0$)

ΔB_z = Mean value of $B_z(o)$ over the interval τ

$$\equiv \tau^{-1} \int_{t_1}^{t_2} B_z(o,t)\,dt$$

The results of the calculations are shown in Figs.9-13.

It will be noted that ΔB_z is linearly dependent on I_{max} but is almost independent of B_{zmax} (except when $B_{zmax} \lesssim B_\theta(r_o)$). By reference to the appendix and to Fig.4 it will be seen that ΔB_z is

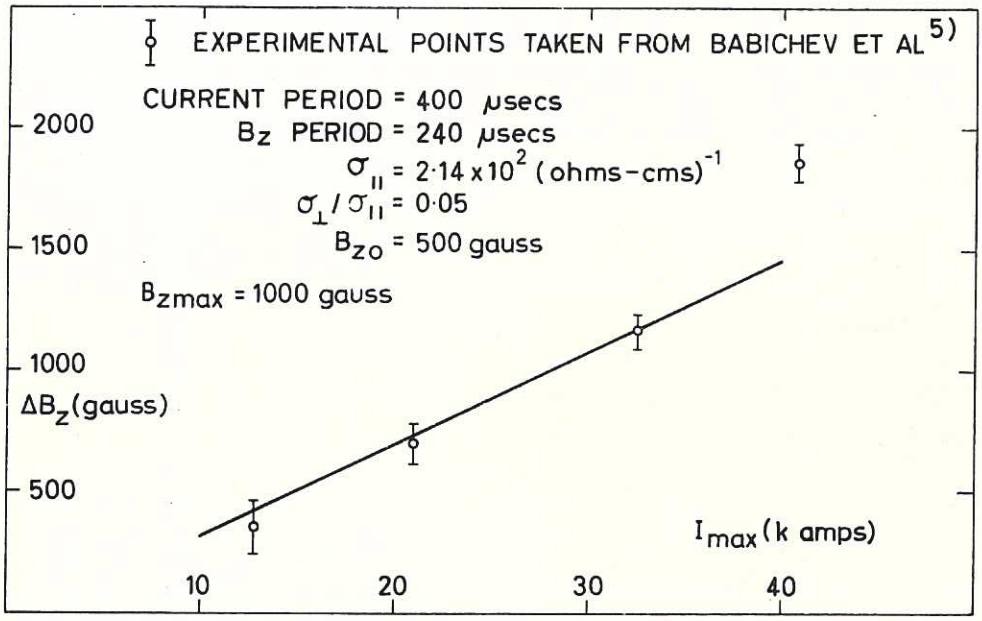

Fig. 9

The theoretical (full line) and experimental (points) dependence of ΔB_z on I_{max}. The experimental points are taken from Babichev et al. (footnote 5)

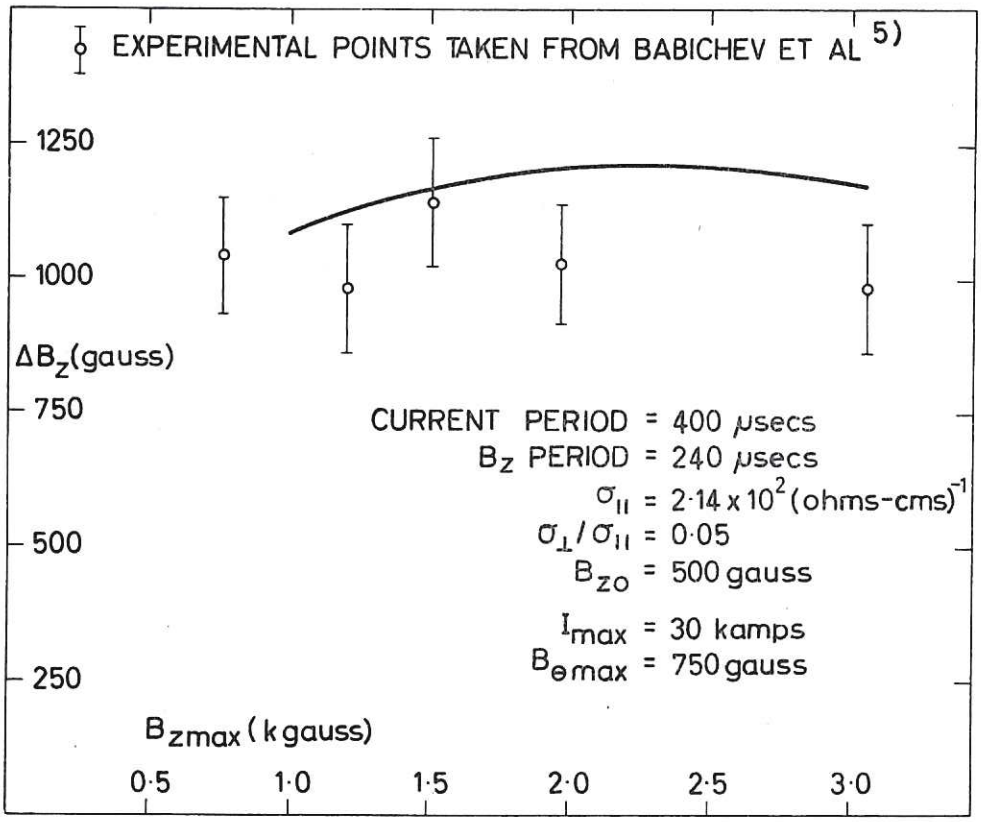

Fig. 10

The theoretical (full line) and experimental (points) dependence of ΔB_z on B_{zmax}. The experimental points are taken from Babichev et al. (footnote 5)

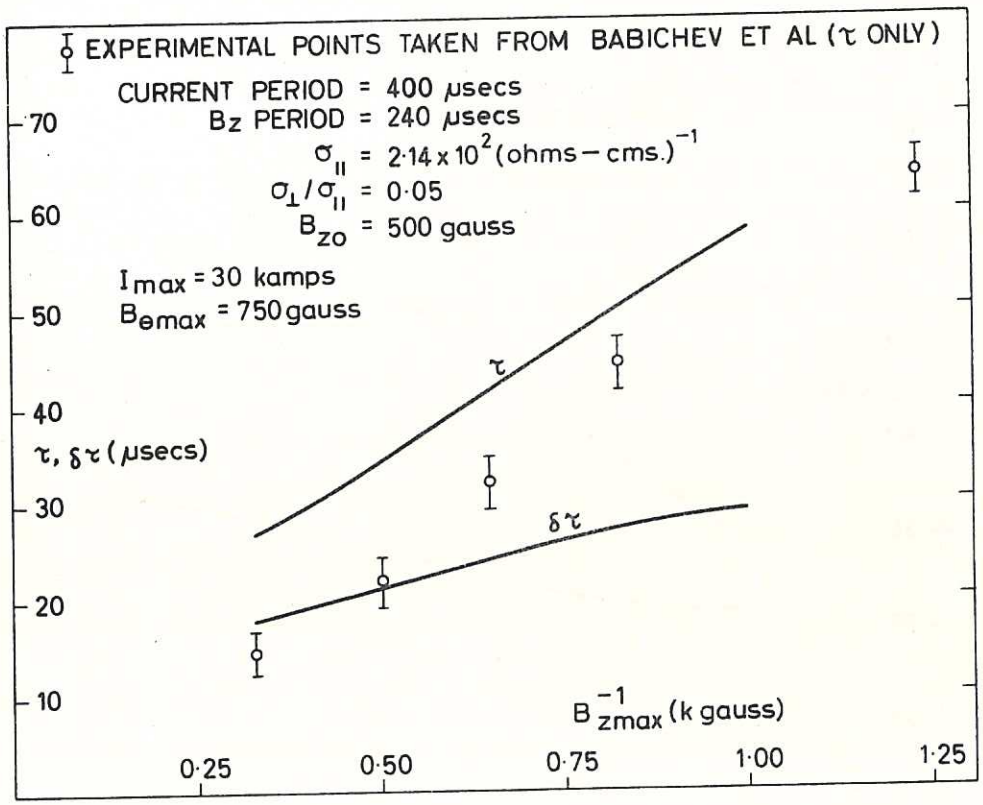

Fig. 11

The theoretical (full lines) and experimental (points) dependence of τ and $\delta\tau$ on B_{zmax}^{-1}. The experimental points for τ are taken from Babichev et al. (footnote 5)

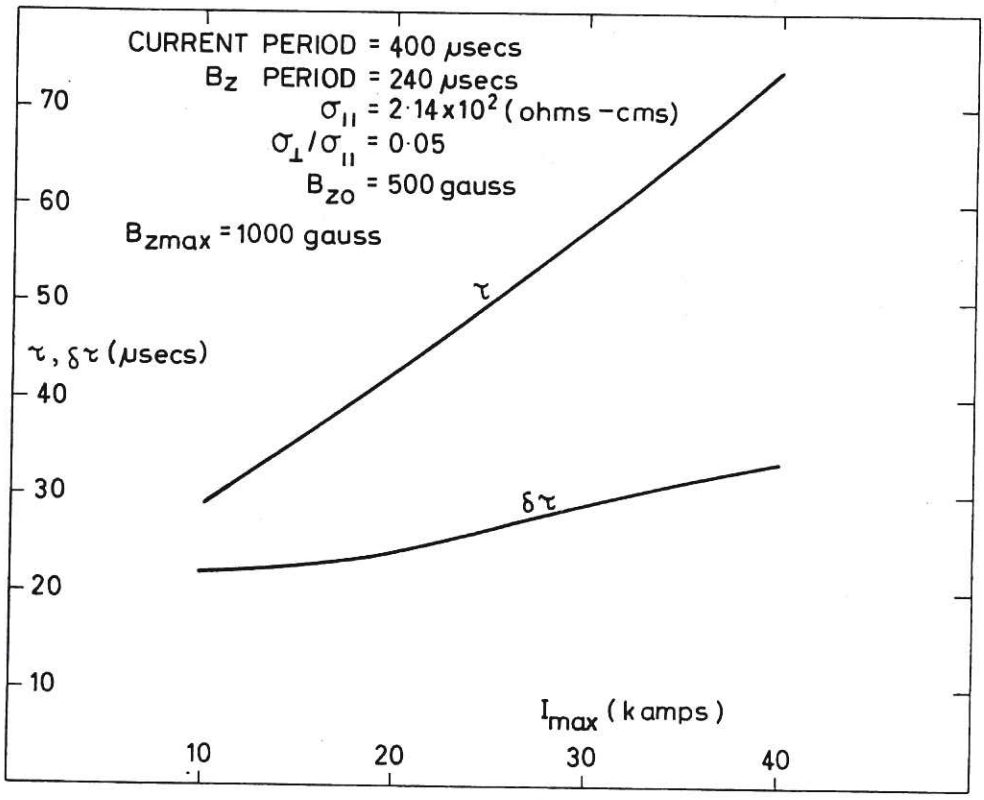

Fig. 12

The theoretical dependence of τ and $\delta\tau$ on I_{max}

determined primarily by the value of the fields $B_\theta(r_o)$ and $B_z(r_o)$ when they became equal. Thus for a specific value of B_{zmax} an approximately linear dependence on I_{max} would be expected, approximate only, due to the slight variation of t_1 with I_{max}. The effect of varying B_{zmax}, keeping I_{max} constant, would not be expected to be very great. Some effect should be observed due, as in the preceding example, to the dependence of t_1 on the rate of change of $B_z(r_o)$, i.e. on B_{zmax}. If the parameters had been such that $B_\theta(r_o)$ had varied more rapidly in time there would have been a stronger dependence of ΔB_z on B_{zmax}. The proximity of the experimental points to the computed curves is very encouraging although it must be pointed out that it has been assumed that the former were obtained in a similar manner to the calculated values of ΔB_z. The agreement shown in Fig.9 would appear, at first sight, to be a little fortuitous since reference to the original oscillograms[5] shows the current to be anything but sinusoidal during the end of the second quarter cycle. However, a closer examination shows that the rapid reversal of B_z at the centre is always over before the current deviates significantly from a basically sinusoidal shape.

The interval $\delta\tau$ is moderately insensitive to both B_{zmax} and I_{max}, varying by approximately 50% for a factor four change in either. As outlined in the appendix, $\delta\tau$ should be determined predominantly by σ_{11}. The bulk of the variation observed here is due to a residual coupling between the B_θ and B_z fields resulting in a modification of the simple diffusion picture discussed in section 2(iv). That $\delta\tau$ is still proportional to σ_{11} is borne out by Fig.13 in which the results of a further series of calculations are plotted, all parameters except σ_{11} being maintained constant.

The parameter τ is very nearly linearly dependent on B_{zmax}^{-1} and I_{max}. Its magnitude is composed of two parts : $\delta\tau$ and the

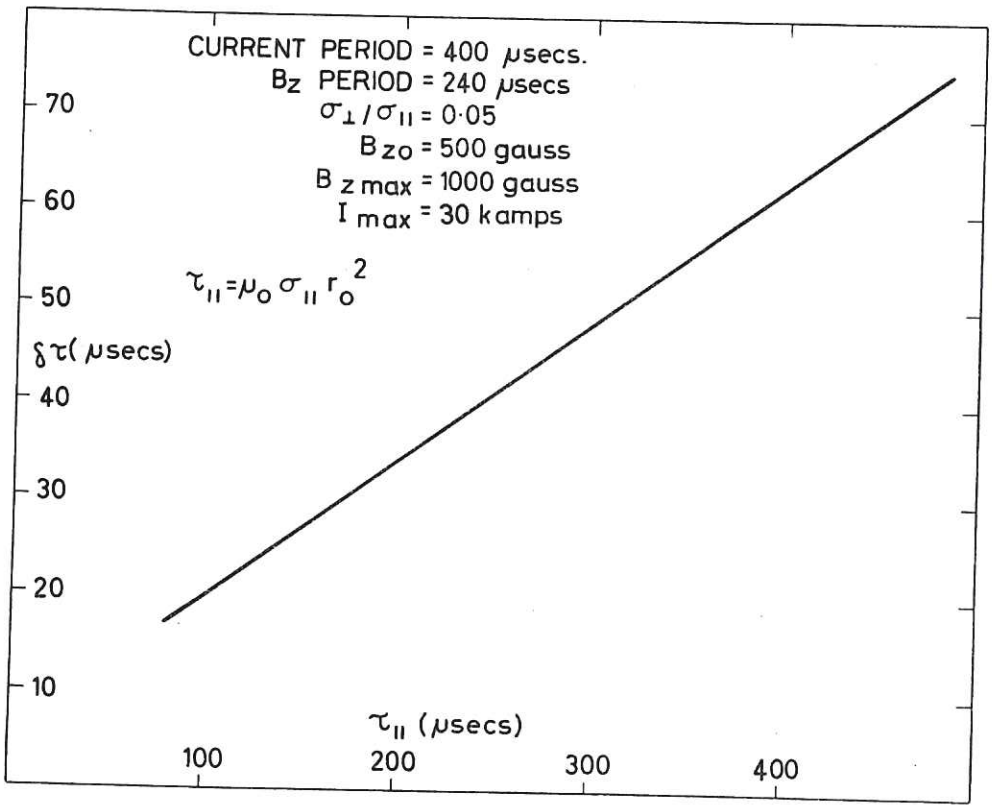

Fig. 13

The theoretical dependence of $\delta\tau$ on the parallel diffusion time τ_{11}

time taken for $B_z(r_o)$ to fall from a value $B_\theta(r_o)$ to zero. The former has already been discussed. The latter is, by definition, proportional to I_{max} and inversely proportional to B_{zmax}, hence even if $\delta\tau$ were invariant, τ would be expected to have the observed behaviour. In fact only $\delta\tau$, not τ , has any real physical significance. The agreement with experiment is not this time so good. The calculated values of τ are of course dependent on the value of σ_{11} adopted. The value used throughout these calculations was chosen to correspond to an electron temperature of 5 eV - this being the lowest temperature quoted for the experiments. Undoubtedly a better choice could have been made, but whether it would have been any more significant is debatable.

5. CONCLUSIONS

The main purpose of this paper has been to discuss the theory of a simple plasma model defined by Maxwell's equations and the Ohm's law (4) and to show how, in the near force free limit, the investigation of time dependent solutions is able to explain, in a consistent manner, a set of experimentally observed facts both qualitatively and, to a large extent, quantitatively. It is important to note at this point just what is to be understood by the word "explain" in the preceding sentence. In the strict sense this paper does not explain the experiments - that is, in fundamental physical terms. What it does do is to show that the same phenomena can be predicted for the particularly simple model discussed. It does not exclude the possibility that other, perfectly justifiable, models might be equally successful* and it does not attempt to answer the more important questions

*The following publication has appeared since the writing of this paper: A.P. Babichev, A.I. Karchevskii, Ya.A. Muromkin. Zhur. Eksp. i Teoret. Fiz., 43, 881, (1962).

such as, for example, why does current flow only along field lines? It does however, strongly suggest that these are questions well worth asking, and indeed, attempts have already been made to find the answers, by Kadomtsev[14] , for example.

Finally, the conclusions drawn as a result of this study can be stated as follows:-

1. The full time-dependent theory, in the limit $\sigma_\perp/\sigma_{11} \ll 1$, is able to predict, both qualitatively and quantitatively, all the phenomena observed and reported during the programmed reversal of the axial magnetic field in a slow pinch discharge.
2. Since there is no particular reason to believe that this experiment is, in principle, different to many others, it is reasonable to predict that the theory discussed might be equally successful in interpreting other transient situations arising in cylindrical (or, to an approximation, toroidal) pinch discharges.
3 Care must be exercised in using a continuous set of steady state solutions to represent a transient situation. This is particularly so if the limit $\sigma_\perp/\sigma_{11} \rightarrow 0$ is being considered and if the ratio of axial to azimuthal fields at any point becomes appreciably less than unity.

ACKNOWLEDGEMENTS

The author wishes to express his sincere thanks to Dr. A.A. Ware for initially suggesting the possibilities of this investigation and for a number of encouraging discussions and useful ideas.

The assistance and encouragement of a number of members of the Theoretical Division, Culham Laboratory is gratefully acknowledged. In particular that of Dr. K.V. Roberts and Dr. K. Hain

(of the Institute for Plasma Physics, Garching, Munich) for the use of their subroutine "FIELD1" with which the integration of the diffusion equations was carried out; Mr. K.J. Whiteman for supplying most of the data for Fig.1; Dr. R.J. Tayler (now at Corpus Christi College, Cambridge) for access to some of his early unpublished work on this subject; and Miss J. Baker for supplying valuable programming assistance.

APPENDIX

THE PHYSICAL INTERPRETATION OF THE NUMERICAL RESULTS

This appendix discusses in detail the physical processes giving rise to the theoretically observed phenomena. In order to simplify much of the discussion it is convenient to consider the limit $\sigma_\perp/\sigma_{11} \equiv 0$. As stated previously the results that have been presented are for $\sigma_\perp/\sigma_{11} = 0.05$ and this is sufficiently small for the force free limit to be a good approximation. However, at some points, it will be necessary to recall that $\sigma_\perp$ is not exactly zero, but only small.

With these considerations in mind Eq.(5) to (10) can be written in the form

$$\frac{\partial E_z}{\partial r} = \frac{\partial B_\theta}{\partial t} \quad , \tag{A.1}$$

$$\frac{1}{r}\frac{\partial}{\partial r}(rE_\theta) = -\frac{\partial B_z}{\partial t} \quad , \tag{A.2}$$

$$j_z = \frac{1}{\mu_o}\frac{1}{r}\frac{\partial}{\partial r}(rB_\theta) = \sigma_{11}\frac{B_z}{B^2}\left[B_z E_z + B_\theta E_\theta\right] \tag{A.3}$$

and

$$j_\theta = -\frac{1}{\mu_o}\frac{\partial B_z}{\partial r} = \sigma_{11}\frac{B_\theta}{B^2}\left[B_z E_z + B_\theta E_\theta\right]. \tag{A.4}$$

Equation (A.2) can be written in the alternative form

$$E_\theta(r) = -\frac{1}{r}\frac{\partial \phi_z(r)}{\partial t} \quad , \tag{A.5}$$

where

$$\phi_z(r) = \int_o^r r' B_z(r')\, dr'$$

and is proportional to the axial flux contained within a cylinder of radius r.

During the period preceding the point A (Fig.4), $B_z(r_o) > B_\theta(r_o)$ and all field variation is moderately slow. Under these conditions it is to be expected that the field configurations will be given by a continuous series of steady state solutions in which, by virtue of Eq. (A.1) and (A.2), E_z is spatially uniform and E_θ

is zero. That this is so, is borne out by the agreement shown in Fig.4.

When $B_z(r_o)$ becomes less than $B_\theta(r_o)$ the fields will still tend to diffuse to the steady state configurations characterised by these boundary values. Thus, after passing through a minimum, $B_z(o)$ will tend to increase more and more rapidly ($\sigma_\perp/\sigma_{11}$ being sufficiently small). The resulting rapid build-up of axial flux near the centre generates an E_θ which is zero at the centre, large and negative just off-centre, and which tends to zero or a small positive value near the wall (total flux decreasing). This field opposes the j_θ arising directly from the steady state fields, the net result being that the rapid rise of B_z at the centre is inhibited. The degree to which $B_z(o)$ can overcome this constraining influence depends on the magnitude of the coupling between E_θ and j_θ. Reference to Eq.(17) shows that this is determined, near the centre ($B_\theta < B_z$), by σ_{11} , or by $\sigma_\perp$ if $\sigma_\perp/\sigma_{11} \sim 1$. Thus, as would be expected, since the fields are attempting to relax to steady state configurations, the shorter the diffusion times the more time, relatively speaking, $B_z(o)$ has to attain large values and the higher it rises.

When B_z becomes small near the wall, either positively or negatively, the magnetic field lines become almost perpendicular to the z axis and the resistance to the axial current in that region is high. Since the total current remains essentially unaltered, a greater fraction of it must be carried near the centre. The cross-sectional area decreases as r^2 and hence the enhancement of the central current density is large. As B_z in the outer regions increases more negatively the axial resistance there decreases. Meanwhile the annulus of small B_z, i.e. high axial resistance, moves into the central region resulting in an effective

switching of the axial current from the centre to the outside. During this period a very large E_z (i.e. driving voltage) is built up at $r = r_o$ which falls rapidly when the current reverts to the outer region.

Since the gradient of B_z is large in the neighbourhood of its zero as it approaches the centre, the annulus of high resistivity becomes thin and is responsible for the sharp minimum occurring in j_z. A large j_z at the centre demands a B_θ increasing with radius. A small or negative j_z in an adjacent region demands a B_θ decreasing with radius. These can only exist simultaneously if B_θ is peaked, the maximum being situated between the regions.

In this way the calculated transient field configurations can be made physically plausible. In addition the following argument can be used to provide a little more information on the behaviour of the fields as the B_z zero approaches $r = 0$. If B_z vanishes at $r = \bar{r}$ and $\bar{r} \ll r_o$, $B_z(r)$ and $E_\theta(r)$ can be approximated near the centre by

$$B_z(r) \approx B_z(o)\ (1 - r/\bar{r})$$

and

$$E_\theta(r) \approx E'_\theta\ r \quad ,$$

where

$$E'_\theta = \partial E_\theta / \partial r \text{ at } r = 0 \ .$$

Then

$$\mu_o\ j_z = \frac{1}{r}\frac{\partial}{\partial r}(rB_\theta) = \frac{\mu_o\ \sigma_{\shortparallel}\ B_z(o)\ E'_\theta}{B_\theta(r)}\ r(1 - \frac{r}{\bar{r}}) \ ,$$

i.e. j_z changes sign at $r = \bar{r}$. It can be shown that, if $\sigma_\perp/\sigma_{\shortparallel}$ is sufficiently large, this sign change is suppressed.

Integrating from 0 to r yields

$$B_\theta(r) = \left[\frac{\mu_o\ \sigma_{\shortparallel}\ \bar{r}^2\ B_z(o)\ E'_\theta}{2}\right]^{\frac{1}{2}} \frac{r}{\bar{r}}\ (1 - \frac{4r}{5\bar{r}})^{\frac{1}{2}} \ ,$$

from which it can be deduced that B_θ has a peak centred approximately about $r = \bar{r}$, of height and width proportional to $\bar{r}$.

Thus the reversed j_z and B_θ peak, decreasing in height and width as it approaches the centre (Fig.7), are purely local phenomena associated with the zero in B_z.

It may have been noted that, at F in Fig.8, j_z reverses near the wall. This is due to the so-called "Inverse Skin Effect"[9] induced by the total axial current approaching zero.

The time $\delta\tau$ taken for the zero in B_z to move from the wall to the centre can be interpreted by reference to Section 2(iv). There it was shown that in the neighbourhood of $B_z/B_\theta = 0$, i.e. at $r = \bar{r}$, B_z diffuses with a characteristic time determined by σ_{11}. Although this will not be true very close to $r = 0$, where $B_\theta \longrightarrow 0$, it would still be reasonable to expect $\delta\tau$ to be proportional to τ_{11}. This is confirmed by Fig.13 which shows the results of repeating one of the previous calculations with different values of σ_{11}, keeping $\sigma_\perp/\sigma_{11}$ constant.

In addition it was also shown that B_θ could diffuse with a rate determined by $\sigma_\perp$. This explains how B_θ at $r = \bar{r}$ is able to vary so rapidly as $\bar{r}$ moves inwards.

During much of the interval $\delta\tau$, $B_z(o)$ is increasing but, as the B_z zero approaches the centre, it finally succumbs and falls rapidly. The rate at which it does so is determined (Section 2(iii)) by $\sigma_\perp$ since at the centre, before the B_z zero actually reaches there, $B_\theta/B_z = 0$. In this way it is possible to account for the rapidity of the reversal of B_z at the centre.

With B_z of the same sign at all radii the field configurations soon relax again to those given by steady state theory.

REFERENCES

1. D.J. LEES and M.G.RUSBRIDGE. "Proceedings of the Fourth International Conference on Ionization Phenomena in Gases, vol.II, 954,(North Holland Publishing Company, Amsterdam, 1960).
2. H.K. FORSEN, A.A. SCHUPP and A.A. WARE. Phys. Rev., 125, 417, (1962).
3. A.P. BABICHEV, A.I. KARCHEVSKII, YU.A. MUROMKIN and V.V. SOKOL'SKII. Soviet Physics - JETP, 14, 983,(1962).
4. M.G. RUSBRIDGE and D.J. LEES. Magnetic Field Configurations in High Current Discharges. Atomic Energy Research Establishment Report. AERE-R 3304, (1960).
5. A.P. BABICHEV et al. International Conference on Plasma Physics and Controlled Nuclear Fusion, Salzburg, Sept. 1961, paper 215 (Associated Electrical Industries translation AEI T/1721).
6. A.A. WARE. Private Communication.
7. W. MARSHALL. Kinetic Theory of an Ionized Gas. Atomic Energy Research Establishment Reports. AERE -T/R 2247, 2352, 2419, (1960).
8. J.H. ADLAM and R.J. TAYLER. The Diffusion of Magnetic Fields in a cylindrical conductor. Atomic Energy Research Establishment Memo.. AERE-T/M 160,(1958).
9. M.G. HAINES. Proc. Phys. Soc., 74, 576,(1959).
10. G.D. HOBBS. Magnetic Field Configurations in Rigid Toroidal Conductors carrying Time-dependent currents. Culham Laboratory Report. CLM-R 15,(1961).
11. R.J. BICKERTON. Proc. Phys. Soc., 72, 618,(1958).
12. K. HAIN. Pinch Collapse. Atomic Energy Research Establishment Report. AERE-R 3383,(1961).

13. L. SPITZER. Physics of Fully Ionized Gases. (Interscience Publishers, Inc., New York, 1956).

14. B.B. KADOMTSEV. International Conference on Plasma Physics and Controlled Nuclear Fusion, Salzburg, Sept. 1961, paper 227 (Associated Electrical Industries Translation AEI T/1718).